Elsevier Editorial System(tm) for Applied Energy
Manuscript Draft

Manuscript Number: APEN-D-15-04263R1

Title: Analysis and comparison of Integrated Solar Combined Cycles using parabolic troughs and linear Fresnel reflectors as concentrating systems

Article Type: Original Paper

Keywords: Integrated Solar Combined Cycle (ISCC); combined cycle; Concentrating solar power (CSP); parabolic trough collector (PTC); linear Fresnel reflector (LFR)

Corresponding Author: Dr. Antonio Rovira, Doctor

Corresponding Author's Institution: UNED

First Author: Antonio Rovira, Doctor

Order of Authors: Antonio Rovira, Doctor; Rubén Barbero; María J Montes, Doctor; Rubén Abbas, Doctor; Fernando Varela, Doctor

Abstract: This paper compares the annual performance and economic feasibility of Integrated Solar Combined Cycles (ISCC) using two solar concentration technologies: parabolic trough collectors (PTC) and linear Fresnel reflectors (LFR). Integration of solar energy to the steam turbine of a combined cycle gives some advantages: the first one is the fuel saving due to the solar contribution and, additionally, the second one is that this contribution takes place especially in highly insolated periods with high ambient temperatures, when conventional combined cycles decrease their power rate and work with decreased efficiency.
Previous works showed the convenience of ISCC using PTC and direct steam generation in locations with severe climatology. Besides, LFR technology is currently considered as a good option for reducing the cost of concentrating solar power. Thus, in the present work both concentrating technologies are studied and compared. Solar contribution is only used for evaporating water, increasing the production of the high pressure level of the steam generator. Two locations, Almeria and Las Vegas, are selected for the annual analyses. Results show that the proposed evaporative configurations increase the annual performance. Also, the thermal contribution is higher with PTC, but LFR may improve the economic feasibility of the plant.

# Analysis and comparison of Integrated Solar Combined Cycles using parabolic troughs and linear Fresnel reflectors as concentrating systems

**Antonio Rovira[(1), *]; Rubén Barbero[(1)] ; María José Montes[(1)], Rubén Abbas[(2)]; Fernando Varela[(1)]**

*Corresponding author: rovira@ind.uned.es

[(1)]UNED, Depto. Ingeniería Energética, ETS Ingenieros Industriales

[(2)]Universidad Politécnica de Madrid, Depto. Ingeniería Energética, ETSII

## Abstract

This paper compares the annual performance and economic feasibility of Integrated Solar Combined Cycles (ISCC) using two solar concentration technologies: parabolic trough collectors (PTC) and linear Fresnel reflectors (LFR). Integration of solar energy to the steam turbine of a combined cycle gives some advantages: the first one is the fuel saving due to the solar contribution and, additionally, the second one is that this contribution takes place especially in highly insolated periods with high ambient temperatures, when conventional combined cycles decrease their power rate and work with decreased efficiency.

Previous works showed the convenience of ISCC using PTC and direct steam generation in locations with severe climatology. Besides, LFR technology is currently considered as a good option for reducing the cost of concentrating solar power. Thus, in the present work both concentrating technologies are studied and compared. Solar contribution is only used for evaporating water, increasing the production of the high pressure level of the steam generator. Two locations, Almeria and Las Vegas, are selected for the annual analyses. Results show that the proposed evaporative configurations increase the annual performance. Also, the thermal contribution is higher with PTC, but LFR may improve the economic feasibility of the plant.

**Key words:** Integrated Solar Combined Cycle (ISCC), combined cycle, Concentrating solar power (CSP), parabolic trough collector, linear Fresnel reflector.

**Nomenclature**

| | |
|---|---|
| Symbols | |
| CCGT | Combined Cycle Gas Turbine |
| *CELF* | Constant-escalation levelization factor (-) |
| *CF* | Concentration factor (-) |
| *CF'* | Geometrical concentration factor (-) |
| CSP | Concentrating solar power |
| *D* | Diameter (m) |
| *DNI* | Direct normal irradiation (W $m^{-2}$) |
| DSG | Direct steam generation |
| *E* | Energy (J) |
| *FiT* | Feed-in tariff (€ $J^{-1}$) |
| $H_c$ | Heating value (J $Kg^{-1}$) |
| HRSG | Heat Recovery Steam Generator |
| *HR* | Heat rate (-) |
| ISCC | Integrated solar combined cycles |
| *L* | Length (m) |
| *LC* | Levelized cost (€) |
| *LCOE* | Levelized cost of energy (€ $J^{-1}$) |
| LFR | Linear Fresnel reflectors |
| $\dot{m}_f$ | Fuel mass flow (kg $s^{-1}$) |
| *p* | Selling price of the energy (€ $J^{-1}$) |
| *P* | Power (W) |
| PTC | Parabolic trough collector |
| $\dot{Q}$ | Thermal power (W) |
| *T* | Temperature (K) |
| | |
| Greek letters | |
| $\alpha$ | Absorptivity (-) |
| $\Delta$ | Increment |
| $\eta$ | Efficiency (-) |
| $\eta_{net,inc,solar}$ | Net incremental solar efficiency (-) |
| $\eta_{opt}$ | Optical efficiency (-) |
| $\eta_t$ | Thermal efficiency (-) |
| $\tau$ | Transmissivity (-) |
| | |
| Subscripts | |
| *amb* | Ambient |
| GT | Gas turbine |
| inv | Investment |
| min | Minimum |
| O&M | Operation and maintenance |
| *sat* | Saturation |
| SC | Steam cycle |

## 1. Introduction

At the short and medium terms, concentrating solar power (CSP) is going to share scenario with conventional thermal power plants. In such context, integrated solar combined cycles (ISCC) may become an interesting choice for power generation because hybridisation can provide an efficient use of the fossil and solar resources, better than using solar dedicated and conventional power plants separately.

At high power rate levels (several hundreds of MW), combined cycle gas turbines (CCGT) are the most efficient thermal-to-mechanical energy conversion systems. Therefore, they have been deeply studied and commercially installed as the core of the power plants since several decades ago. As examples of studies focused to increase the efficiency of CCGT stand those carried by Bassilly [1-3], Franco and Casarosa [4] or Polyzakis et al. [5].

Besides, a significant amount of solar thermal power plants have been lately installed throughout the world. Most of the installed plants use parabolic trough collector technology (PTC), and minority central tower receivers [6]. More recently, linear Fresnel reflectors (LFR) have been also installed. Nowadays, PTC is implemented using collectors like Eurotrough and Solargenix, and it may be considered as a well proven technology. On the other side, LFR had a late development compared to PTC, but it seems to have some potential to reduce the Levelized Cost of Energy (LCOE) in concentrating solar power, thanks to its design that involves many degrees of freedom [6-8] and allows efficiency improvement [9, 10] and reduced acquisition costs [11,12].

Hybridisation of solar energy with combined cycles provides some synergies during the yearly operation. In fact, the most demanding conditions for CCGT technology correlate well to the optimal ambient conditions for CSP, which favour the integrated behaviour and efficiency of the ISCC [13-15]. Previous works [16, 17] showed the convenience of ISCC using PTC and direct steam generation (DSG) in locations with hard climatology, but economic feasibility is questionable in other climates [13]. In Ref. [18], several ISCC configurations were studied in order to find the best point for adding the solar contribution in the heat recovery steam generator (HRSG), finding that the best choice is to evaporate water with DSG at the high pressure level without pre-heating or superheating. Ref. [19]

shows similar conclusions, and authors propose a configuration with DSG in all the pressure levels even removing the evaporators of the HRSG. The same authors also propose the inclusion of a solar multiple in the solar field in order to increase the yearly solar contribution [20]. Finally, a comprehensive literature review is done in [21], focused on the works that consider PTC as solar concentrating technology, but not other options like LFR.

On the other hand, the study of ISCC coupled to LFR has not been carried out up to now. This integration has been previously suggested [22], although in that work the performance was not assessed. In Ref. [23], authors suggest a hybridisation for preheating water before evaporation although in conventional Rankine power plants instead of in combined cycles. Comparisons of PTC and LFR have been presented for solar-only power plants: Refs. [24-26] show the technical feasibility and the breaking cost of the LFR to be competitive; in Ref. [27] authors show that LFR produces higher thermal power than PTC given a fixed land area; and Ref. [28] suggests that technical and economical improvements are possible in LFR technology although nowadays the thermal performance of PTC is higher. It is expected that such good features of LFR in pure solar power plants may be extrapolated to ISCC, thus, the comparison of LFR and PTC in ISCC is required.

Therefore, the objective of the paper is the comparison in terms of yearly production and generation cost of ISCC working with PTC and LFR technologies. In the proposed configurations, solar contribution is dedicated to the water evaporation at the high pressure level of the HRSG, with neither preheating nor superheating, as it advised in Ref. [18]. Both technologies are characterised and simulated in two locations: Almeria and Las Vegas.

## 2. Studied configurations

The studied configurations consist of 2x1 combined cycles, with two gas turbines and two dual pressure level HRSGs that feed a steam turbine. Solar contribution is included by means of a PTC or a LFR solar field. In both cases, receivers directly produce steam from saturated water that comes from the corresponding high pressure level drum of the HRSG. Therefore, the solar field works in parallel to the high pressure level evaporators of the HRSGs.

Figures 1 and 2 depict the sketch of both configurations. In addition, two extra configurations are defined as the references: a conventional HRSG without solar contribution; and a reference ISCC similar to the one analysed in Refs. [13, 16], using PTC and DSG that preheat and evaporate water of the high pressure level of the HRSG. The schematics are shown in figures 3 and 4, respectively.

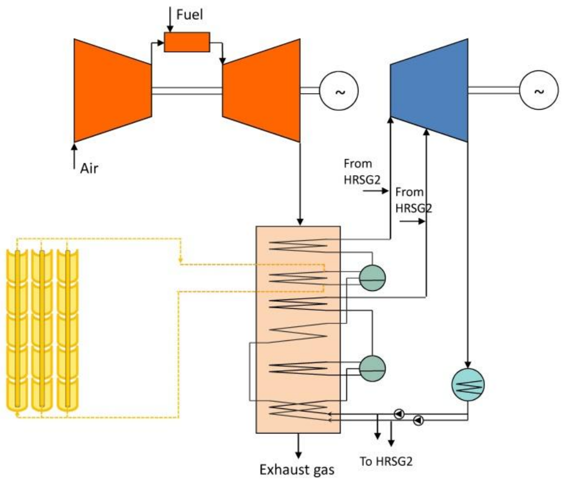


Figure 1: Proposed only-evaporative PTC ISCC.

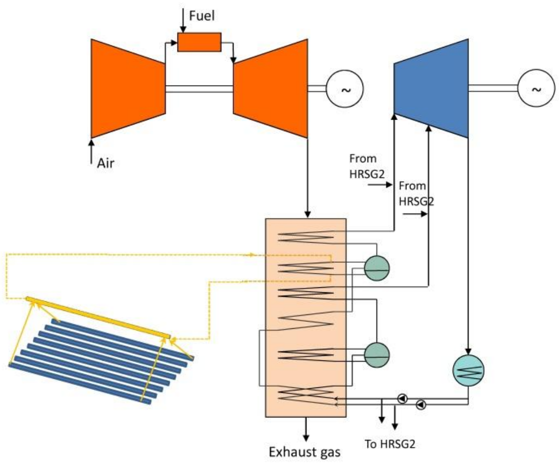


Figure 2: Proposed only-evaporative LFR ISCC.

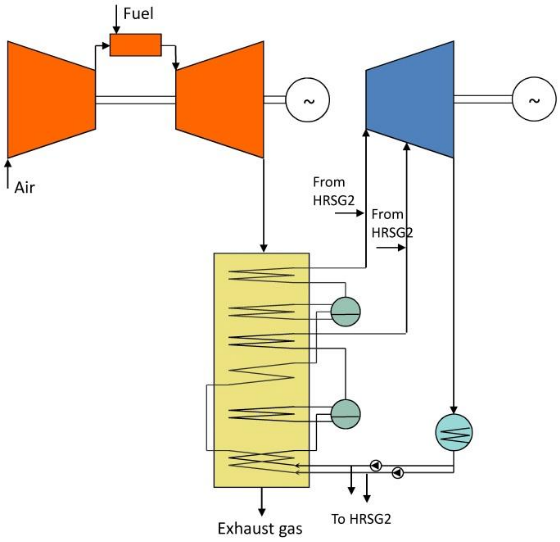


Figure 3: Reference CCGT.

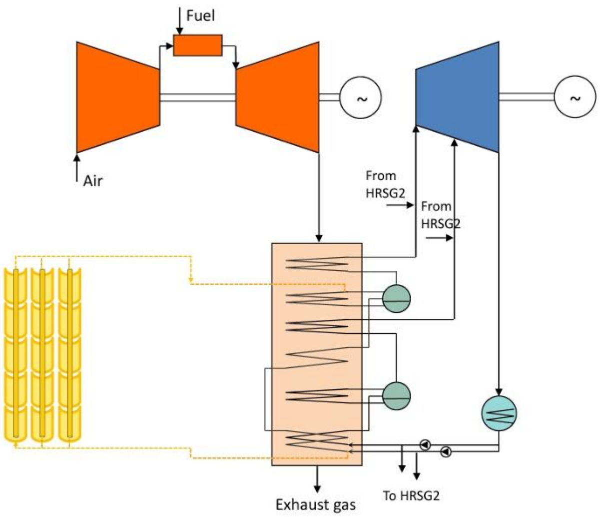


ç

Figure 4: Reference PTC ISCC.

Table 1 presents the data used for of the gas turbine, HRSG and steam cycle, that are the same in all configurations. Data related to the solar fields are given in the next section.

Table 1. Technical data of the combined cycle at nominal conditions

| | |
|---|---|
| Ambient conditions | 288.15 K, 1 bar |
| Compression ratio | 16:1 |
| Air mass flow | 210 kg/s |
| Fuel mass flow | 31 kg/s |
| Turbine inlet temperature | 1450 K |
| Turbine outlet temperature | 828 K |
| Gas turbine power rate | 72.6 MW |
| Gas turbine efficiency | 35.1 |
| Compressor isentropic efficiency | 85 % |
| Gas turbine isentropic efficiency | 90 % |
| Combustion chamber efficiency | 98 % |
| Natural gas lower heating value | 48 MJ/kg |
| High pressure steam temperature | 818 K |
| High pressure | 90 bar |
| High pressure pinch point | 10 K |
| Low pressure steam temperature | 566 K |
| Low pressure | 5 bar |
| Low pressure pinch point | 10 K |
| Steam turbine isentropic efficiency | 87 % |
| Pump efficiency | 75 % |
| Electro-mechanical efficiency | 94 % |
| Reference CCGT power rate | 226 MW |
| Reference CCGT efficiency | 54.6 % |

## 3. Methodology and simulation models

The simulation models for the CCGT and the PTC were developed in previous works [13, 16]. They are based on the mass and energy balances applied to each component of the power plant. These models allow the simulation of the power plant at the design point and also at off-design conditions. In the case of the CCGT components, once these balances are established and solved for the design condition, the nominal performance may be obtained and each component may be characterised (characteristic curves, heat exchange surface, etc.). This characterisation, together with the new mass and energy balances at the off-design conditions, allows the simulation at different ambient and part load conditions. In the case of the PTC solar field, the balances allow the solar field sizing, in terms of number of unitary collectors in series for each row of parabolic troughs and number of rows in parallel to obtain the required thermal power, as well as the off-design simulation.

Parabolic trough design is the Eurotrough-150, although the absorber tube thickness is higher due to a higher pressure than that of the synthetic oil. It was shown in Ref. [18] that, in order to contribute with 50 $MW_{th}$ to the steam cycle (25 $MW_{th}$ to each HRSG), the reference ISCC configuration requires 82632 $m^2$ of reflectors in about 260000 $m^2$ of land. These reflective surface and use of land are maintained in the only-evaporative PTC configuration. The geometrical and optical parameters of the PTC configurations are shown in table 2.

The solar field efficiency of the reference ISCC reaches a value of 71.3%. In the case of the only-evaporative PTC configuration, the solar field efficiency drops to 67.1% due to the higher mean working temperature. Despite this efficiency decrease, performance of the HRSG increases significantly (as shown in Ref. [18]) and overcomes that disadvantage (see section 6).

The design points considered for the solar field in Almeria and Las Vegas are shown in table 3. In such conditions, the PTC solar field supplies 25 $MW_{th}$ to each HRSG in the reference PTC ISCC and 23.6 $MW_{th}$ in the only-evaporative PTC ISCC. However, as suggested and discussed in Ref. [13], the HRSG and the steam turbine are sized considering only a half of this thermal power surplus. The equipment is not sized for the full thermal power surplus due to the fact that the solar field and HRSG & steam turbine are not simultaneously at nominal conditions over the year, since high irradiation correlates to ambient temperatures higher than the nominal one of the conventional combined cycle.

Table 2. Geometrical and optical parameters for the collector loop considered

| | |
|---|---|
| *Geometrical parameters for the collector loop* | |
| Absorber tube outer diameter | 0.07 m |
| Absorber tube inner diameter | 0.055 m |
| Glass envelope outer diameter | 0.115 m |
| Glass envelope inner diameter | 0.109 m |
| Module length | 12.27 m |
| Mirror length in every module | 11.9 m |
| *Optical parameters for the collector ET-150* | |
| Intercept factor | 0.92 |
| Mirror reflectivity | 0.92 |
| Glass transmissivity | 0.945 |
| Solar absorptivity | 0.94 |
| Peak optical efficiency | 0.75 |
| Thermal emissivity | 0.04795 + 0.0002331 T(ºC) |
| *Nominal operating conditions* | |
| Mass flow per loop | 1.44 kg/s |

Table 3. Design points of the solar fields in Almeria and Las Vegas.

| Design point parameter | Almeria | Las Vegas |
|---|---|---|
| DNI (W/m$^2$) | 850 | 900 |
| Altitude (m) | 366 | 664 |
| Longitude (º) | 2º 21’ W | 115º 10’ W |
| Latitude (º) | 35º 05’ N | 36º 04’ N |
| Ambient temperature (K) | 298 | 298 |
| Incidence angle (N-S) (º) | 13º 39’ | 12º 38’ |

Finally, for this work the simulation models of LFR and the CCGT have been integrated. Again, the objective of these models is the simulation of the plant at on- and off-design conditions, as well as the sizing and characterization of the equipment. As mentioned in section 1, the number of degrees of freedom in the design of the solar field and receivers of LFR technology is high. In order to simplify the analysis without carrying out an optimisation, for this work the geometrical layout of Fresdemo [29] was considered, both for the reflector fields and the linear receiver. The main features are shown in table 4.

Table 4. Geometrical parameters of the LFR

| | |
|---|---|
| Module length | 100 m |
| Module width | 21 m |
| Receiver height | 10 m |
| Tube diameter | 0.14 m |
| Number of mirror rows | 25 |
| Mirror width | 0.6 m |
| Mirror height | 2 m |

Once the geometry is selected, the following step is the determination of the thermal power impinging on the receiver and the thermal efficiency, which allows the calculation of the thermal power supplied to the steam. The impinging thermal power was assessed by means of ray trace using the Monte Carlo methodology. This model, implemented in Matlab, is based on the generation of 100000 rays from the sky to the reflectors at each calculation step. Some operations are applied to the rays: reflections of the rays on the mirrors towards the receiver, several Gaussian errors due to the manufacturing and tracking systems and the consideration of a solar disc intensity to follow the model given by Buie et al. [30]. The LFR ray-trace model is described in detail in [10] and it was applied successfully in [7, 9, 10]. In this work, it was used to characterize the concentration factor on the receiver as a function of the longitudinal and transversal angles of incidence. This concentration is depicted in figure 5.

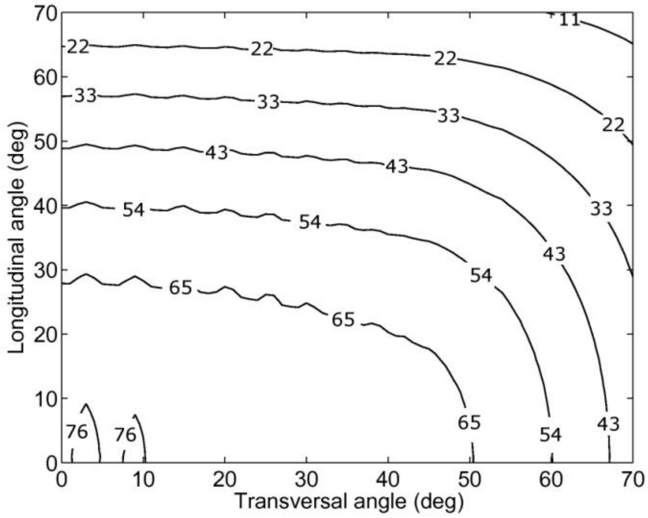


Figure 5: Concentration factor depending on the impining transversal and longitudinal angles.

Once the concentration is known at any moment, the incident thermal power is obtained as the product of this concentration factor and the modified DNI (including the incidence angle modifier), taking into account the absortivity of the tube and the transmisivity of the glass:

$$P_{tube} = DNI \cdot CF \cdot \alpha \cdot \tau = DNI \cdot CF' \cdot D \cdot L \cdot \eta_{opt} \tag{1}$$

Where $CF$ is the actual concentration factor, $\alpha$ the tube absorptivity (0.93), $\tau$ the transmissivity of the glass (0.94), $CF'$ the geometrical concentration factor and $D$ and $L$ the diameter and tube length.

The thermal power transferred to the steam is calculated with the power impinging on the tube and the thermal efficiency of the receiver. In this work, the following equation was used [29]:

$$\eta_t = \eta_{opt} - 0{,}0366 \cdot \frac{T_{sat} - T_{amb}}{DNI} - 0{,}000707 \cdot DNI \cdot \left( \frac{T_{sat} - T_{amb}}{DNI} \right)^2 \tag{2}$$

Where $T_{sat}$ is the saturation temperature, $T_{amb}$ the ambient temperature and the optical efficiency ($\eta_{opt}$) is calculated taking into account the second equality of equation 1.

In order to obtain steam with a quality of 30% at a suitable velocity inside the tube (lower than 8 m/s), 3 modules of 100 m are required. The efficiency at a saturation temperature of 303 ºC (90 bar) is 89.5 %. Therefore, 24 loops in parallel of 3 modules each one are required to produce 50 $MW_{th}$ of steam. In the LFR case, the land requirement is 151200 $m^2$, and the reflective area of the mirrors is 90720 $m^2$.

Like in PTC configurations, the HRSG and steam turbine of the ISCC are sized taking into account only a half of the thermal energy surplus supplied by the solar field at its design conditions. The nominal power rate of the ISCC configurations is about 233 $MW_e$.

## 4. Annual simulations.

When all the components of the solar field and the combined cycle are characterised, the performance may be calculated at any working condition. In the mentioned previous works, annual simulation were carried out on hourly basis, taking into account the ambient conditions (including solar time and DNI) each hour of the year, which leads to 8760 calculating points. For the present work the methodology was changed in order to reduce the computation time. This change involves the analysis of the climatic year and the discretisation of the ambient conditions with the objective of finding operating conditions systematically repeated over the year. Specifically, for the PTC configuration, it was studied how often the values of modified DNI are repeated for each interval of ambient temperatures. Six different intervals of modified DNI - ambient temperature were studied to find the most suitable grid: 1ºC - 10W/$m^2$; 1ºC - 20W/$m^2$; 1ºC - 50W/$m^2$; 2ºC - 10W/$m^2$; 5ºC - 10W/$m^2$; and 2ºC - 20W/$m^2$.

Figure 6 shows, as an example, the frequency matrix obtained for the case of 2ºC - 20W/$m^2$ intervals in Almeria. The yearly performance of the reference ISCC using all these intervals differs less than a 0.2%, as shown in table 5. Due to the good agreement of the results using the different grids, it was selected the matrix of 2ºC - 20W/$m^2$ intervals, which results in 538 calculating points for Almeria and 909 for Las Vegas, instead of 8760.

Table 5. Number of points and yearly production with the different discretisations. Reference ISCC.

| | Almeria | | Las Vegas | |
|---|---|---|---|---|
| | E (GWh) | Points | E (GWh) | Points |
| 1ºC - 10W/$m^2$ | 1875.87 | 1568 | 1881.18 | 2393 |
| 1ºC - 20W/$m^2$ | 1875.81 | 954 | 1881.03 | 1560 |
| 1ºC - 50W/$m^2$ | 1875.83 | 445 | 1880.98 | 750 |
| 2ºC - 10W/$m^2$ | 1875.79 | 956 | 1880.88 | 1563 |
| 5ºC - 10W/$m^2$ | 1876.48 | 470 | 1881.08 | 755 |
| 2ºC - 20W/$m^2$ | 1875.81 | 538 | 1880.87 | 909 |

The year characterisation for the LFR configuration was analogous, but considering the concentrated irradiance on the receiver (*DNI·CF*), according to figure 5, instead of the modified DNI. The selected interval was 2ºC – 2000W/m$^2$, which leads to 393 and 669 calculating points for Almeria and Las Vegas, respectively. As an example, figure 7 shows the used frequency matrix for the LFR configuration in Almeria.

| W/m$^2$ \ ºC | 5 | 7 | 9 | 11 | 13 | 15 | 17 | 19 | 21 | 23 | 25 | 27 | 29 | 31 | 33 | 35 | 37 |
|---|---|---|---|---|---|---|---|---|---|---|---|---|---|---|---|---|---|
| 0 | 14 | 94 | 297 | 536 | 775 | 788 | 638 | 490 | 460 | 395 | 322 | 181 | 63 | 12 | 5 | 1 | |
| 20 | | 2 | 4 | 10 | 14 | 20 | 23 | 20 | 11 | 14 | 12 | 11 | 9 | | | | |
| 40 | 1 | 3 | 2 | 4 | 8 | 19 | 26 | 19 | 8 | 13 | 2 | 8 | 4 | | | | |
| 60 | 1 | 3 | 4 | 6 | 13 | 15 | 10 | 15 | 8 | 15 | 5 | 8 | 8 | 5 | | | |
| 80 | | 1 | 5 | 3 | 6 | 14 | 22 | 13 | 8 | 12 | 16 | 8 | 3 | 1 | | | |
| 100 | | 1 | 5 | 6 | 10 | 11 | 11 | 17 | 5 | 9 | 5 | 5 | 3 | 1 | 1 | 1 | |
| 120 | | 3 | 1 | 5 | 6 | 15 | 14 | 7 | 9 | 5 | 5 | 11 | 7 | 1 | | | |
| 140 | | 4 | 2 | 6 | 12 | 12 | 16 | 8 | 9 | 6 | 6 | 2 | 4 | 2 | | | |
| 160 | | | 2 | 6 | 4 | 12 | 15 | 16 | 11 | 8 | 8 | 6 | 4 | 1 | | | |
| 180 | | 2 | 3 | 4 | 9 | 12 | 18 | 12 | 8 | 4 | 5 | 7 | 5 | 2 | | | |
| 200 | | 1 | 4 | 6 | 7 | 8 | 18 | 10 | 7 | 9 | 6 | 9 | 4 | 1 | | | |
| 220 | | | 1 | 16 | 7 | 13 | 14 | 11 | 6 | 5 | 4 | 4 | 4 | 5 | | | |
| 240 | | 2 | 7 | 5 | 9 | 13 | 11 | 9 | 6 | 5 | 3 | 4 | 2 | 4 | 1 | | |
| 260 | | 1 | 3 | 1 | 13 | 5 | 16 | 10 | 6 | 12 | 7 | 11 | 11 | | | | |
| 280 | | | 3 | 11 | 10 | 14 | 16 | 10 | 7 | 10 | 5 | 6 | 4 | 2 | | | |
| 300 | 1 | | 5 | 2 | 12 | 11 | 18 | 10 | 11 | 8 | 7 | 4 | 7 | 5 | | | |
| 320 | | | 2 | 7 | 11 | 12 | 8 | 18 | 9 | 13 | 10 | 5 | 6 | 7 | 1 | | 1 |
| 340 | | | 3 | 8 | 6 | 12 | 11 | 15 | 5 | 11 | 9 | 8 | 4 | 5 | 1 | | |
| 360 | | | 2 | 5 | 8 | 8 | 5 | 12 | 8 | 8 | 10 | 5 | 3 | 1 | | | |
| 380 | | | 1 | 6 | 3 | 7 | 18 | 11 | 10 | 5 | 7 | 9 | 2 | 1 | | | |
| 400 | | | 2 | 4 | 7 | 16 | 7 | 18 | 9 | 14 | 9 | 3 | 4 | 4 | | | |
| 420 | | | | 4 | 5 | 9 | 19 | 13 | 12 | 9 | 9 | 4 | 7 | 3 | | | |
| 440 | | | 1 | 1 | 5 | 5 | 11 | 20 | 15 | 15 | 12 | 10 | 6 | 2 | | | |
| 460 | | | 1 | 1 | 6 | 13 | 19 | 15 | 11 | 9 | 11 | 8 | 12 | 3 | 1 | | |
| 480 | | | 2 | 1 | 3 | 4 | 13 | 12 | 10 | 6 | 22 | 5 | 5 | 3 | | | |
| 500 | | | 1 | | 5 | 4 | 19 | 23 | 8 | 13 | 17 | 9 | 6 | 6 | 1 | | |
| 520 | | | | | | 6 | 10 | 15 | 12 | 14 | 17 | 6 | 6 | 7 | | | |
| 540 | | | 1 | 1 | 2 | 7 | 10 | 11 | 10 | 10 | 20 | 9 | 15 | 4 | | | |
| 560 | | | | | 1 | 5 | 6 | 11 | 12 | 9 | 16 | 24 | 9 | 1 | 1 | 1 | |
| 580 | | | | 1 | 3 | 6 | 15 | 13 | 10 | 13 | 15 | 7 | 8 | 6 | 1 | | |
| 600 | | | | 1 | 1 | 3 | 10 | 13 | 12 | 10 | 13 | 18 | 16 | 4 | 1 | | 1 |
| 620 | | | | 1 | | 4 | 13 | 11 | 10 | 8 | 11 | 14 | 7 | 9 | | 1 | 1 |
| 640 | | | | 2 | 1 | 2 | 9 | 11 | 3 | 7 | 9 | 8 | 7 | 7 | | 1 | |
| 660 | | | | | 2 | 2 | 3 | 11 | 8 | 8 | 6 | 6 | 5 | 3 | 2 | | |
| 680 | | | | | | 2 | 7 | 8 | 6 | 13 | 13 | 12 | 5 | 4 | 1 | 1 | |
| 700 | | | | | | 2 | 8 | 9 | 14 | 10 | 14 | 15 | 6 | 7 | | 1 | |
| 720 | | | | | 1 | 1 | 3 | 14 | 12 | 9 | 11 | 8 | 10 | 4 | | | |
| 740 | | | | | 1 | 1 | 4 | 7 | 8 | 12 | 8 | 9 | 8 | 1 | | | 1 |
| 760 | | | | | | 1 | 2 | 3 | 2 | 5 | 9 | 11 | 3 | 3 | 1 | 1 | 1 |
| 780 | | | | 1 | 2 | | 2 | 4 | 5 | 8 | 7 | 6 | 6 | 5 | 3 | 1 | |
| 800 | | | | | | 1 | 5 | 3 | 6 | 4 | 7 | 1 | 9 | | 5 | 1 | |
| 820 | | | | | | | | 2 | 5 | 3 | 6 | 5 | 3 | | | 2 | |
| 840 | | | | | | 1 | 1 | 3 | 2 | 5 | 9 | 3 | 2 | 1 | | 1 | |
| 860 | | | | | | | 2 | 1 | 2 | 3 | 3 | 1 | 2 | | 3 | 1 | |
| 880 | | | | | | | 2 | 1 | 2 | 2 | 3 | 1 | | | 2 | | |
| 900 | | | | | | | | | 2 | 4 | | | | | | | |
| 920 | | | | | | | | | | | | | | | | | |
| 940 | | | | | | | | | | | 1 | | | | | | |

Figure 6. Frequency matrix of modified DNI-temperature for Almería for PTC.

| kW/m² \ ºC | 5 | 7 | 9 | 11 | 13 | 15 | 17 | 19 | 21 | 23 | 25 | 27 | 29 | 31 | 33 | 35 | 37 |
|---|---|---|---|---|---|---|---|---|---|---|---|---|---|---|---|---|---|
| 0 | 17 | 115 | 355 | 603 | 859 | 896 | 789 | 630 | 543 | 488 | 385 | 226 | 104 | 29 | 8 | 3 | |
| 2 | | 1 | 1 | 6 | 12 | 17 | 25 | 26 | 5 | 16 | 12 | 12 | 4 | 2 | | | |
| 4 | | | | 8 | 14 | 15 | 15 | 13 | 14 | 13 | 12 | 16 | 11 | 3 | | | 1 |
| 6 | | | 1 | 9 | 10 | 14 | 13 | 14 | 8 | 15 | 13 | 7 | 7 | 5 | | | |
| 8 | | | | 4 | 5 | 16 | 14 | 15 | 6 | 16 | 16 | 14 | 10 | 4 | 1 | | |
| 10 | | | 1 | 7 | 5 | 9 | 24 | 14 | 14 | 14 | 16 | 9 | 15 | 6 | 1 | | |
| 12 | | | 1 | 8 | 6 | 11 | 13 | 18 | 21 | 8 | 7 | 16 | 7 | 5 | | | |
| 14 | | | 2 | 5 | 12 | 9 | 27 | 17 | 10 | 9 | 10 | 9 | 8 | 5 | 1 | | |
| 16 | | | 1 | 1 | 5 | 11 | 15 | 12 | 9 | 12 | 7 | 9 | 11 | 5 | 1 | | |
| 18 | | | | 4 | 5 | 8 | 14 | 24 | 12 | 14 | 9 | 9 | 5 | 4 | 2 | | |
| 20 | | | 2 | 2 | 5 | 10 | 16 | 10 | 8 | 10 | 16 | 10 | 7 | 5 | | 1 | 1 |
| 22 | | | | 1 | 10 | 4 | 14 | 17 | 9 | 7 | 9 | 11 | 5 | 2 | | | |
| 24 | | | | 1 | 5 | 7 | 11 | 11 | 8 | 8 | 13 | 3 | 9 | 3 | | | |
| 26 | | | | | 5 | 6 | 7 | 18 | 13 | 8 | 9 | 5 | 8 | 8 | | 1 | |
| 28 | | | | 5 | 5 | 6 | 14 | 18 | 10 | 7 | 13 | 13 | 10 | 2 | | | |
| 30 | | | 1 | 1 | 4 | 7 | 7 | 10 | 5 | 8 | 11 | 11 | 5 | 4 | | | |
| 32 | | | | | 2 | 9 | 9 | 8 | 17 | 11 | 11 | 14 | 8 | | 1 | | |
| 34 | | | | 2 | 3 | 6 | 11 | 9 | 10 | 11 | 15 | 8 | 3 | 9 | 1 | | |
| 36 | | | | 1 | 3 | 5 | 9 | 13 | 13 | 4 | 15 | 5 | 4 | 5 | 1 | 1 | 1 |
| 38 | | | | 1 | 1 | 4 | 12 | 9 | 3 | 6 | 16 | 14 | 9 | 8 | | 1 | |
| 40 | | | | | 4 | 4 | 8 | 15 | 10 | 13 | 18 | 10 | 11 | 4 | 1 | | |
| 42 | | | | | 1 | 7 | 5 | 16 | 10 | 9 | 7 | 11 | 12 | 1 | | | |
| 44 | | | | 1 | 2 | 4 | 4 | 6 | 8 | 13 | 5 | 7 | 5 | 3 | | | |
| 46 | | | | | 3 | 5 | 9 | 6 | 10 | 10 | 13 | 10 | 7 | 5 | 1 | 1 | 2 |
| 48 | | | | | | 7 | 5 | 5 | 13 | 6 | 11 | 9 | 7 | 5 | 1 | 1 | |
| 50 | | | | | 1 | 3 | 4 | 3 | 5 | 6 | 9 | 9 | 5 | 2 | 4 | 2 | |
| 52 | | | | | | | 9 | 7 | 5 | 10 | 11 | 9 | 8 | 3 | | 1 | |
| 54 | | | | | | 3 | 7 | 1 | 3 | 7 | 6 | 8 | 5 | 3 | | | |
| 56 | | | | | 2 | 4 | 4 | 6 | 2 | 9 | 5 | 6 | 5 | 2 | | | |
| 58 | | | | | | 4 | 3 | 1 | 3 | 6 | 2 | 4 | 5 | 1 | 1 | 1 | |
| 60 | | | | | | 2 | 1 | 2 | 2 | 5 | 11 | 4 | 1 | | | 1 | |
| 62 | | | | | | | 4 | 4 | 5 | 4 | 11 | 1 | 2 | | 4 | | |
| 64 | | | | | | | 3 | 3 | 1 | 2 | 5 | 5 | 1 | | 1 | | |
| 66 | | | | | | | 1 | 3 | | 5 | 1 | 1 | | | 1 | | |
| 68 | | | | | | 1 | 3 | 1 | 2 | | 1 | 1 | 1 | | | | |
| 70 | | | | | | | | | 1 | 2 | | | | | | | |

Figure 7. Frequency matrix of modified DNI·CF-temperature for Almería for LFR.

The minimum threshold for the solar contribution is set to 300 W/m$^2$ for the PTC configurations and 600 W/m$^2$ for the LFR one, higher than that of the PTC case because lower values usually corresponds to low solar height, which leads to high shading losses and low concentration factors.

To assess the performance of the different configurations, several figures of merit have been used, as well as the annual production of energy. The thermal efficiency of the ISCC is calculated as the ratio of the produced power to the thermal power supplied by the fuel and the solar field:

$$\eta = \frac{P_{GT} + P_{SC}}{\dot{m}_f \cdot H_c + \dot{Q}_{net-solar}} \quad (3)$$

However, the thermal efficiency is not the best parameter to evaluate ISCC power plants, since it decreases as the solar contribution increases because solar heat is supplied to the bottoming cycle. Nevertheless, solar energy contributes to save fossil fuel because it increases the power generation without associated fuel consumption. The fuel saved thanks to the solar contribution can be assessed using a heat rate (*HR*) ratio, which is the inverse of the efficiency for the CCGT configuration and it should decrease for the ISCC ones:

$$HR = \frac{\dot{m}_f \cdot H_c}{P_{GT} + P_{SC}} \tag{4}$$

Finally, the net incremental solar efficiency may be used to compare the solar-to-electricity conversion efficiency of ISCC and solar pure power plants:

$$\eta_{net,inc,solar} = \frac{(P_{GT} + P_{SC})_{ISCC} - (P_{GT} + P_{SC})_{CCGT}}{\dot{Q}_{net,solar}} \tag{5}$$

Besides, the performance of the solar field may be compared using the thermal efficiency of the field:

$$\eta_{solar\ field} = \frac{\dot{Q}_{net,solar}}{DNI \cdot A_{col}} \tag{6}$$

## 5. Economic analysis

In the economic analysis, the levelized cost of energy (LCOE) for each considered configuration and emplacement is assessed. In order to compare adequately the generation cost of a solar and fossil hybrid system, an escalation rate factor for the fuel cost is required. The factor is needed because the cost of solar energy has only the amortisation and the operation & maintenance components but not a fuel consumption one, which entails some advantage over fossil technology.

The levelized cost is calculated with the following equation:

$$LCOE = \frac{LC_{inv} + LC_{O\&M} + LC_{fuel}}{E_{annual}} \tag{7}$$

The levelized cost of the investment ($LC_{inv}$) is the product of the total investment and the capital-recovery factor [31], which depends on the interest rate and the life of the power plant. The levelized costs of operation & maintenance (O&M) and fuel depends on the O&M and fuel costs, respectively, and the constant-escalation levelization factors (CELF) that, in turn, depends on the respective escalation rates [31].

In addition to the LCOE, the solar marginal cost ($C_{marg}$) of the solar contribution is assessed, as it provides information regarding the generation cost due to the solar field. It is defined as below:

$$C_{marg} = \frac{\left(LC_{inv} + LC_{O\&M} + LC_{fuel}\right)_{ISCC} - \left(LC_{inv} + LC_{O\&M} + LC_{fuel}\right)_{CCGT}}{\Delta E_{annual}} \tag{8}$$

The parameters considered for the economic analysis are presented in table 6. For the LFR technology two economic scenarios are proposed, one optimistic (lower cost of the equipment) and another conservative (higher costs). The definition of several scenarios is usual for this technology [25, 32, 33] due to the lack of actual data and the small number of power plants based on this technology.

Table 6. Economic data.

| | |
|---|---|
| Specific land cost | 2 €/m$^2$ |
| Specific cost for the PTC | 200 €/m$^2$ |
| Specific cost for the LFR | 80 €/m$^2$ (optimistic)<br>160 €/m$^2$ (conservative) |
| Surcharge for construction, engineering and contingencies | 10 % |
| Specific cost for the power block from [13, 34] | (466.1 + 113900/P[MW]) €/kW |
| Solar field O&M cost | 9 €/(year·kW) |
| Combined cycle O&M cost | 17,9 €/(year·kW) |
| O&M equipment cost percentage of investment per year | 1 % |
| Interest rate | 4 % |
| Life | 25 years |
| O&M Escalation rate | 1% |
| Fuel escalation rate | 2.5 % |
| Price of natural gas | 2.32 c€/kWh |

## 6. Results

Table 7 shows the results obtained for the two proposed configurations (evaporative PTC and LFR) as well as those obtained for the reference PTC ISCC and the reference CCGT. One may observe that the yield of all the ISCC configurations is higher than the one obtained by the reference CCGT, thanks to the solar contribution.

Table 7. Results of the annual simulations.

| | Reference CCGT | | Reference PTC ISCC | | Evaporative PTC ISCC | | Evaporative LFR ISCC (conservative/optimistic) | |
|---|---|---|---|---|---|---|---|---|
| | Almeria | Las Vegas | Almeria | Las Vegas | Almeria | Las Vegas | Almeria | Las Vegas |
| $E_{fuel}$ (GWh) | 3493 | 3474 | 3493 | 3474 | 3493 | 3474 | 3493 | 3474 |
| $E_{annual}$ (GWh) | 1857 | 1846 | 1876 | 1881 | 1889 | 1900 | 1871 | 1873 |
| HR | 1.88 | 1.88 | 1.86 | 1.85 | 1.85 | 1.83 | 1.87 | 1.85 |
| $E_{sol\_gross}$ (GWh) | - | - | 107.5 | 166.5 | 108.4 | 166.7 | 84.3 | 125.3 |
| ΔE (GWh) | - | - | 19 | 35 | 32 | 54 | 14 | 27 |
| $\eta_{net\ inc\ solar}$ | - | - | 17.7% | 21.0% | 29.5% | 32.4% | 16.6% | 21.5% |
| Investment (M€) | 241.4 | 241.4 | 264.0 | 264.0 | 264.0 | 264.0 | 261.6 / 253.6 | 261.6 / 253.6 |
| $LC_{inv}$ (M€) | 15.45 | 15.45 | 16.9 | 16.9 | 16.9 | 16.9 | 16.7 / 16.2 | 16.7 / 16.2 |
| $LC_{O\&M}$ (M€) | 9.0 | 9.0 | 10.6 | 10.6 | 10.6 | 10.6 | 9.9/9.8 | 9.9/9.8 |
| $LC_{fuel}$ (M€) | 139.4 | 138.6 | 139.4 | 138.6 | 139.4 | 138.6 | 139.4 | 138.6 |
| LCOE (c€/kWh) | 8.82 | 8.84 | 8.89 | 8.83 | 8.83 | 8.74 | 8.87 / 8.84 | 8.82 / 8.79 |
| $C_{mar}$ (c€/kWh) | - | - | 15.86 | 8.61 | 9.42 | 5.58 | 15.4 / 10.9 | 7.97 / 5.66 |

It is also observed that the annual production of the proposed evaporative PTC configuration is higher than that of the reference ISCC. This increase is due to the more efficient use of the solar resource (annual net incremental solar efficiency), which is caused by the lower irreversibility in the HRSG (as it is shown in Ref. [18]) when the solar thermal power is only used to evaporate the water.

On the other hand, it is shown that LFR may work successfully in an ISCC. However, the yearly production of the LFR configurations is lower than those obtained with the PTC, due to its lower performance and solar concentration along the year.

Regarding the location, ISCC configurations emplaced in Las Vegas reach better thermal performance than those emplaced in Almeria, owing to the harder climate and consequently higher solar contribution.

The LCOE obtained is very similar for all configurations because the major contribution to the energy production comes from the fossil resource through the CCGT power plant, while the solar contribution is marginal (below 3% yearly). For that reason, it is advisable not only to analyse the LCOE but also to compare the solar marginal cost to the LCOE. At this regard, when the marginal cost is lower than the LCOE, the solar contribution becomes profitable and, on the contrary, higher solar marginal costs make the solar contribution unadvisable. Also, it is important to note that the results depend strongly on the economic scenario and that a high accuracy is only possible using actual data instead of costing models.

From an economic point of view, the reference PTC ISCC reduces the LCOE in Las Vegas, since the solar marginal cost is always lower than the LCOE, but not in Almeria, where the conventional CCGT has a slightly better behaviour and the solar field has a worse performance. The proposed evaporative PTC ISCC improves the results and makes the ISCC comparable to the reference CCGT in Almeria.

Finally, despite the lower production of the LFR, the economic results are better than those of the reference PTC even in the conservative scenario, and they are close to that of the evaporative PTC ISCC if the optimistic scenario is considered. In fact, the land requirement and the investment are lower than in PTC, and these savings have a significant impact on the amortisation cost, which reduces the LCOE and overcomes the lower annual production.

Figure 8 shows a sensitivity analysis to the fuel cost. It is observed that, in the proposed economic scenario and in Almeria, evaporative PTC ISCC and LFR ISCC (optimistic case) may become an interesting option. However, the reference ISCC and LFR ISCC (conservative case) require high fuel cost to be interesting. In Las Vegas the solar contribution improves the results of all configurations and, particularly, in the evaporative PTC ISCC and LFR ISCC (optimistic case) even at low fuel costs.

The economic scenario might also change in the case of an eventual government support to the solar or ISCC technology. Figure 9 shows the effect on the LCOE and the solar marginal cost of an eventual funding support through government grants applied to the extra investment in the solar field. As observed, with such incentive, at least a grant of a 10% is required in Almeria to make the best ISCC configurations profitable, while it is not required in Las Vegas.

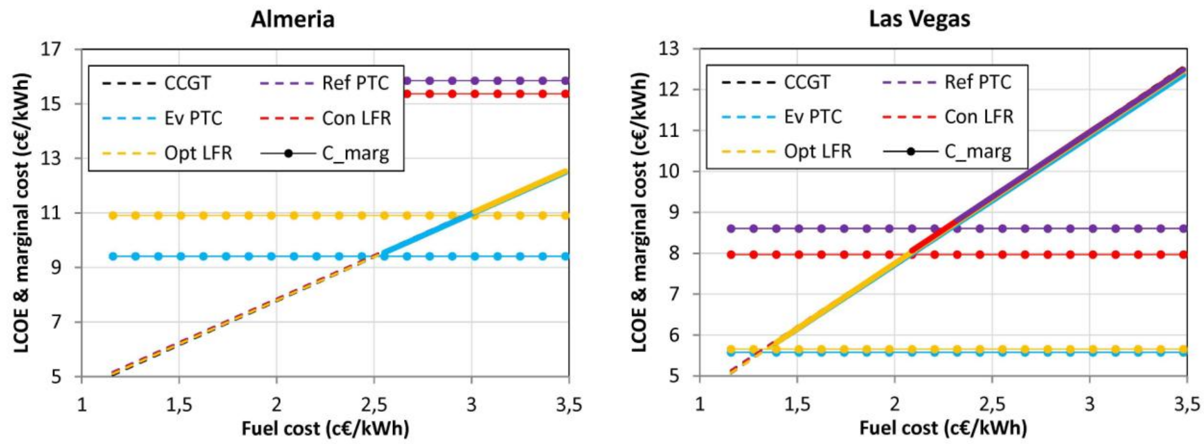


Figure 8. Sensitivity analysis to the fuel cost.

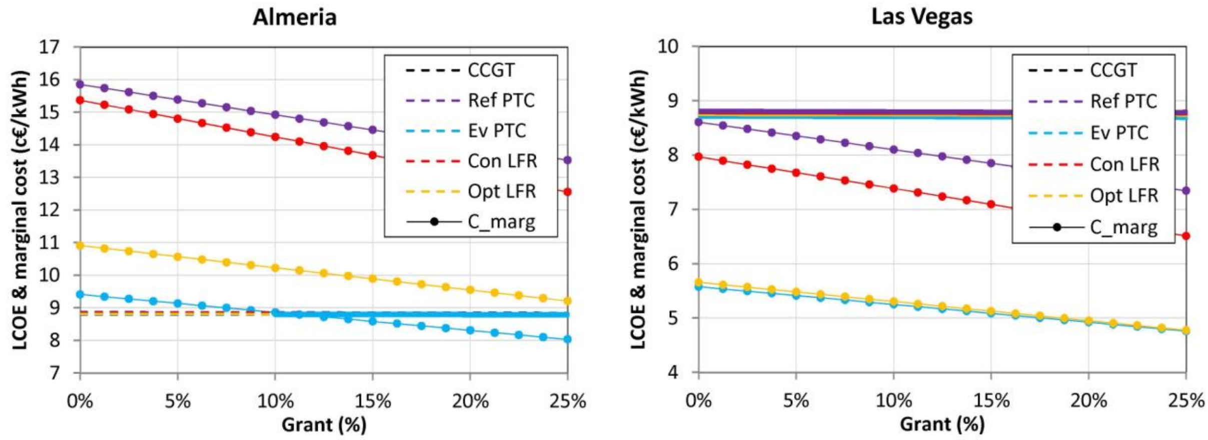


Figure 9. Sensitivity analysis to government support thorugh grants to the solar field investment.

Figure 10 shows the effect of another possible way to support the technology, by means of feed-in tariffs to the solar contribution ($\Delta E_{annual}$). This support improves the economic results through higher incomes instead of lower exploitation costs, as the fixed tariff is higher than the market selling price. In hybrid power plants, like ISCC, this tariff should be applied to the solar incremental power, and the minimum selling price for the energy coming from the fossil resource, which is equivalent to the generation cost once the income surplus has been discounted, may be calculated as below, balancing the incomes to the levelized exploitation cost:

$$p_{\min} \cdot \left(E_{annual} - \Delta E_{annual}\right) + FiT \cdot \Delta E_{annual} = LC_{inv} + LC_{O\&M} + LC_{fuel} \tag{9}$$

In this scenario, the solar contribution is suitable when the solar marginal cost is lower than the feed-in tariff. In the case of Almeria, moderate-to-low support is required to make the best ISCC configurations profitable, needing a feed-in tariff slightly above the reference CCGT LCOE. Again, in Las Vegas such a support is not required, since the marginal cost is always above the tariff.

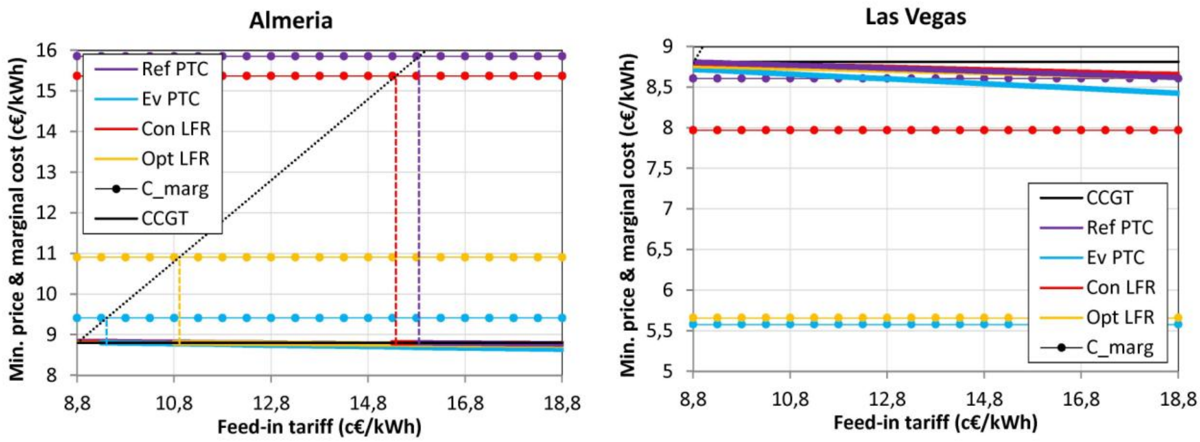


Figure 10. Sensitivity analysis to eventual feed-in-tariffs to the solar contribution.

To sum up, ISCC may be considered as a promising technology specially in emplacements with hard climatology. In addition, it should be note that all these results may be considered as a good starting point for the LFR technology, since LFR solar field has not been optimised for this specific integration. On the contrary, the geometric design of Fresdemo has been replicated to make the simulations. The obtained results suggest that there is some room for improvement, as this technology has many design parameters and, unlike PTC, there is not yet a standardised design. Also, a dedicated development of an ISCC with only-evaporative solar contribution would enhance the thermal performance and the economic results. At this regard, considering DSG for this purpose, LFR technology may have some advantages over PTC, because most of the installed LFR facilities work with DSG.

## 7. Conclusions

This work proposes and compares two integrated solar combined cycles using parabolic trough collector and linear Fresnel reflector technologies. Both configurations generate part of the steam of the high pressure level of the heat recovery steam generator in parallel to the corresponding evaporator. They are also compared to other conventional ISCC and CCGT configurations. Comparisons are made in terms of annual energy production and levelized cost of energy.

The models to simulate the components were developed and integrated in order to assess the behaviour of the ISCC at any operating condition. In addition, a methodology to characterise the year was implemented and used in two emplacements: Almeria and Las Vegas.

From a cost perspective, results show that the proposed evaporative configurations are economically feasible in the studied emplacements, while this is not the case if a solar preheat of water is included, which is only feasible in Las Vegas.

On the other hand, results show that linear Fresnel reflector technology is able to supply steam to the HRSG successfully, although annual production using Fresnel technology is lower than that obtained with parabolic troughs, caused at some extent because the geometry of the receiver has not been optimised for the integration. Additionally, ISCC using Fresnel technology obtains promising economic results considering both optimistic and conservative scenarios.

**Acknowledgements**

Authors acknowledge the financial support of the Spanish Ministry of Economy and Competitiveness to the ENE2012-37950-C02-01 and ENE2012-37950-C02-02 research projects.

## References

[1] Bassily AM. Modeling, numerical optimization, and irreversibility reduction of a triple-pressure reheat combined cycle. Energy, 2007, Vol. 32, pp. 778-794.

[2] Bassily AM. Enhancing the efficiency and power of the triple-pressure reheat combined cycle by means of gas reheat, gas recuperation, and reduction of the irreversibility in the heat recovery steam generator. Applied Energy, 2008, Vol. 85, pp. 1141-1162.

[3] Bassily AM. Numerical cost optimization and irreversibility analysis of the triple-pressure reheat steam-air cooled GT commercial combined cycle power plants. Applied Thermal Engineering 40 (2012) 145-160.

[4] Franco A, Casarosa C. Thermoeconomic evaluation of the feasibility of highly efficient combined cycle power plants. Energy, 2004, vol. 29, pp. 1963-1982.

[5] Polyzakis AL, Koroneos C, Xydis G. Optimum gas turbine cycle for combined cycle power plant. Energy Conversion and Management, 2008, Vol. 49(4), pp. 551–563.

[6] Abbas R, Martínez-Val JM. Analytic optical design of linear Fresnel collectors with variable widths and shifts of mirrors. Renewable Energy, 2015, Vol. 75, pp. 81-92.

[7] Mills DR, Morrison GL. Compact linear fresnel reflector solar thermal power plants. Solar Energy, 2000, vol. 68(3), pp. 263–283.

[8] Montes MJ, Rubbia C, Abbas R, Martínez-Val JM. A comparative analysis of configurations of linear Fresnel collectors for concentrating solar power. Energy, 2014, Vol. 73, pp. 192-203.

[9] Abbas R, Muñoz-Antón J, Valdés M, Martínez-Val JM. High concentration linear Fresnel reflectors. Energy Conversion and Management, 2013, Vol. 72, pp. 60–68.

[10] Abbas R, Montes MJ, Piera M, Martínez-Val JM. Solar radiation concentration features in Linear Fresnel Reflector arrays. Energy Conversion and Management, 2012, Vol. 54, pp. 133–144.

[11] Ford G. CSP: bright future for linear fresnel technology? Renewable energy focus, 2008, Vol. 9(5), pp. 48-51.

[12] Gabbrielli R, Castrataro P, del Medico F, di Palo M, Lenzo B. Levelized cost of heat for linear Fresnel concentrated solar systems. Energy Procedia, 2014, Vol. 49, pp. 1340 – 1349.

[13] Montes MJ, Rovira A, Muñoz M, Martínez-Val JM. Performance analysis of an Integrated Solar Combined Cycle using Direct Steam Generation in parabolic trough collectors. Appl Energ, 2011 vol. 88, pp. 3228–3238.

[14] Antonanzas J, Jimenez E, Blanco J, Antonanzas-Torres F. Potential solar thermal integration in Spanish combined cycle gas turbines. Renewable and Sustainable Energy Reviews, 2014, Vol. 37, pp. 36–46.

[15] Zhu G, Neises T, Turchi C, Bedilion R. Thermodynamic evaluation of solar integration into a natural gas combined cycle power plant. Renewable Energy, 2015, Vol. 74, pp. 815-824.

[16] Montes MJ, Rovira A, Muñoz M, Martínez-Val JM. Proposal of an integrated solar combined cycle system using direct steam generation technology. In: Proc. of 15th int solarPACES symp on sol therm conc technol, Berlin, Germany; 2009.

[17] Antonanzas J, Alia-Martinez M, Martinez-de-Pison FJ, Antonanzas-Torres F. Towards the hybridization of gas-fired power plants: A case study of Algeria. Renewable and Sustainable Energy Reviews 51 (2015) 116–124.

[18] Rovira A, Montes MJ, Varela F, Gil M. Comparison of Heat Transfer Fluid and Direct Steam Generation Technologies for Integrated Solar Combined Cycles. Applied Thermal Engineering, 2013 Vol. 52, pp. 264–274.

[19] Li Y, Yang Y. Thermodynamic analysis of a novel integrated solar combined cycle. Applied Energy 122 (2014) 133–142.

[20] Li Y, Yang Y. Impacts of solar multiples on the performance of integrated solar combined cycle systems with two direct steam generation fields. Applied Energy (2015) http://dx.doi.org/10.1016/j.apenergy.2015.08.094.

[21] Behar O, Khellaf A, Mohammedi K, Ait-Kaci S. A review of integrated solar combined cycle system (ISCCS) with a parabolic trough technology. Renewable and Sustainable Energy Reviews, 2014, Vol. 39, pp. 223–250.

[22] Ordorica-Garcia F, Vidal A, Fernandez A. Novel integration options of concentrating solar thermal technology with fossil-fuelled and $CO_2$ capture processes. Energy Procedia, 2011, Vol. 4, pp. 809–816.

[23] Peterseim JH, White S, Tadros A, Hellwig U. Concentrated solar power hybrid plants, which technologies are best suited for hybridisation? Renewable Energy, 2013, Vol. 57, pp. 520-532.

[24] El Gharbia N, Derbal H, Bouaichaoui S, Said N. A comparative study between parabolic trough collector and linear Fresnel reflector technologies. Energy Procedia, 2011, Vol. 6, pp. (2011) 565–572.

[25] Morin G, Dersch J, Platzer W, Eck M, Häberle A. *Comparison of Linear Fresnel and Parabolic Trough Collector power plants*. Solar Energy, 2012, Vol. 86, pp. 1–12.

[26] Sait HH, Martinez-Val JM, Abbas R, Munoz-Anton J. Fresnel-based modular solar fields for performance/cost optimization in solar thermal power plants: A comparison with parabolic trough collectors, Applied Energy, Volume 141, 1 March 2015, Pages 175-189, ISSN 0306-2619.

[27] Cau G, Cocco D. Comparison of medium-size concentrating solar power plants based on parabolic trough and linear Fresnel collectors. Energy Procedia, 2014, Vol. 45, pp. 101 – 110.

[28] Giostri A, Binotti M, Silva P, Macchi E, Manzolini G. Comparison of two linear collectors in solar thermal plants: parabolic trough versus Fresnel. J. Sol. Energy Eng, 2012, 135(1), 011001. Paper No: SOL-11-1188; doi: 10.1115/1.4006792.

[29] Bernhard R, LaLaing J, Kistner R, Eck M, Eickhoff M, Feldhoff JF, Heimsath A, Hülsey H, Morin G. Linear Fresnel collector demonstration at the psa – operation and investigation. In Proceedings de SolarPACES 2009.

[30] Buie D, Monger A, Dey C. Sunshape distributions for terrestrial solar simulations. Solar Energy, 2003, Vol. 74(2), pp. 113-122.

[31] Bejan A, Tsatsaronis G, Moran M. Thermal Design and Optimization. 1st ed. USA: John Wiley & sons, 1996.

[32] Nixon JD, Davies PA. Cost-exergy optimisation of linear Fresnel reflectors. Solar Energy, 2012, Vol. 86: pp. 147–156.

[33] Zhu G, Wendelin T, Wagner MJ, Kutscher C. History, current state, and future of linear Fresnel concentrating solar collectors. Solar Energy, 2014, Vol. 103: pp. 639–652.

[34] Kehlhofer R, Rukes B, Hannemann F, Stirnimann F. Combined cycle gas-steam turbine power plants. Tulsa, Oklahoma: PennWell, 2009, 3ª ed.